Journal of Thrombosis and Haemostasis, **5**: 2344–2351

IN FOCUS

Role of 'B-b' knob-hole interactions in fibrin binding to adsorbed fibrinogen

C. B. GEER,* A. TRIPATHY,† M. H. SCHOENFISCH,* S. T. LORD*‡ and O. V. GORKUN‡

**Department of Chemistry, University of North Carolina, Chapel Hill, NC; †Department of Biochemistry and Biophysics, University of North Carolina, Chapel Hill, NC; and ‡School of Medicine Department of Pathology and Laboratory Medicine, University of North Carolina, Chapel Hill, NC, USA*

To cite this article: Geer CB, Tripathy A, Schoenfisch MH, Lord ST, Gorkun OV. Role of 'B-b' knob-hole interactions in fibrin binding to adsorbed fibrinogen. *J Thromb Haemost* 2007; **5**: 2344–51.

See also Weisel JW. Which knobs fit into which holes in fibrin polymerization?. This issue, pp 2340–3; Okumura N, Terasawa F, Haneishi A, Fujihara N, Hirota-Kawadobora M, Yamauchi K, Ota H, Lord ST. B:b interactions are essential for polymerization of variant fibrinogens with impaired holes 'a'. This issue, pp 2352–9.

Summary. *Background:* The formation of a fibrin clot is supported by multiple interactions, including those between polymerization knobs 'A' and 'B' exposed by thrombin cleavage and polymerization holes 'a' and 'b' present in fibrinogen and fibrin. Although structural studies have defined the 'A-a' and 'B-b' interactions in part, it has not been possible to measure the affinities of individual knob-hole interactions in the absence of the other interactions occurring in fibrin. *Objectives:* We designed experiments to determine the affinities of knob-hole interactions, either 'A-a' alone or 'A-a' and 'B-b' together. *Methods:* We used surface plasmon resonance to measure binding between adsorbed fibrinogen and soluble fibrin fragments containing 'A' knobs, desA-NDSK, or both 'A' and 'B' knobs, desAB-NDSK. *Results:* The desA- and desAB-NDSK fragments bound to fibrinogen with statistically similar K_d's of 5.8 ± 1.1 μM and 3.7 ± 0.7 μM ($P = 0.14$), respectively. This binding was specific, as we saw no significant binding of NDSK, which has no exposed knobs. Moreover, the synthetic 'A' knob peptide GPRP and synthetic 'B' knob peptides GHRP and AHRPY, inhibited the binding of desA- and/or desAB-NDSK. *Conclusions:* The peptide inhibition findings show both 'A-a' and 'B-b' interactions participate in desAB-NDSK binding to fibrinogen, indicating 'B-b' interactions can occur simultaneously with 'A-a'. Furthermore, 'A-a' interactions are much stronger than 'B-b' because the affinity of desA-NDSK was not markedly different from desAB-NDSK.

Correspondence: Oleg V. Gorkun, Department of Pathology and Laboratory Medicine, University of North Carolina School of Medicine, CB#7525 BBB 816, Chapel Hill, NC 27599-7525, USA.
Tel.: +1 919 966 2617; fax: +1 919 966 6718; e-mail: ovg@med.unc.edu

Received 29 June 2007, accepted 14 September 2007

Keywords: fibrin, fibrinogen, knob-hole interaction, polymerization, surface plasmon resonance.

Introduction

One of the most abundant proteins in blood, fibrinogen plays a pivotal role in hemostasis by sealing vessel ruptures and promoting wound healing [1]. Following vessel injury, soluble fibrinogen is converted to an insoluble fibrin polymer matrix. This conversion occurs in three steps: thrombin catalysis leading to the formation of fibrin monomers; assembly of fibrin monomers into half-staggered, double-stranded protofibrils; and assembly of multiple protofibrils into branched, thick fibers (for review see [2]). The fibrinogen molecule consists of three pairs of non-identical polypeptide chains, Aα, Bβ and γ, linked together by 29 disulfide bonds [3]. Fibrinogen chains are folded into three distinct structural regions, two distal D regions linked by coiled-coil connectors to one central E region (Fig. 1A). Each D region contains polymerization 'a' and 'b' holes located in the C terminus of the γ and Bβ chains, respectively [4–6]. The central E region contains two sets of 'A' and 'B' polymerization knobs that are hidden in fibrinogen [7]. The knobs become exposed only when fibrinogen is transformed into fibrin monomer by the serine protease thrombin. Thrombin removes short peptides, called fibrinopeptides A (FpA) and B (FpB), from the N-terminus of fibrinogen's Aα and Bβ chains, respectively [8]. The newly exposed polymerization knobs of one fibrin monomer interact with corresponding holes of another fibrin monomer or fibrinogen through 'A-a' and 'B-b' knob-hole interactions [9–12].

Thrombin cleaves FpA faster than FpB, so thrombin-catalyzed protofibrils are formed predominantly via 'A-a' interactions [13–15]. Nevertheless, studies with snake venom enzymes that remove only FpA or principally FpB have demonstrated that fibrin clots can be formed by either 'A-a' or 'B-b' interactions, indicating both interactions can mediate protofibril formation [15–20]. Experiments with a variant

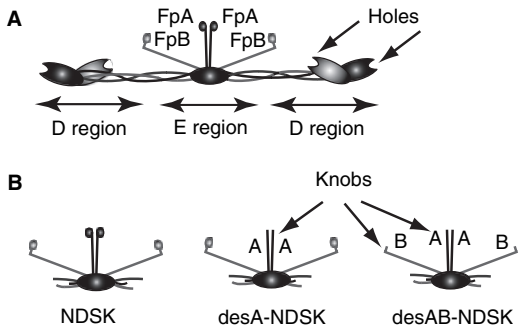

Fig. 1. (A) Schematic representation of fibrinogen; the E and D structural regions and polymerization holes are indicated by arrows, fibrinopeptides A and B (FpA and FpB) are depicted as spheres. (B) Fibrin fragments without (NDSK) and with exposure of polymerization knobs A (desA-NDSK) or A and B (desAB-NDSK).

recombinant fibrinogen showed that 'B-b' interactions may play a substantial role in protofibril formation when 'A-a' interactions are weakened [21]. On the other hand, non-equilibrium based laser tweezers studies by Weisel and co-workers demonstrated that only 'A-a' interactions occur during the binding of fibrin fragments to fibrinogen molecules even when both 'B' knobs and 'b' holes are available [22]. In similar experiments, 'B-b' knob-hole interactions were apparent only when 'A-a' interactions were excluded by experimental design [23]. While it was shown that 'B-b' interactions contribute to overall fibrin clot stability [24,25], the question remains whether 'B-b' interactions occur within protofibrils alongside 'A-a' interactions or between protofibrils.

The work presented herein was designed to measure the strength of 'A-a' interactions under equilibrium conditions and clarify the role of 'B-b' interactions. We used surface plasmon resonance (SPR) to determine the affinity constants of individual knob-hole interactions without interference from other parts of the fibrin molecule that may contribute to polymerization, notably the αC domain and D-D interface [12,26–28]. We measured the binding of fibrin fragments containing either 'A' or 'A' and 'B' knobs (desA-NDSK or desAB-NDSK) to the holes in fibrinogen adsorbed on a hydrophobic surface. We also performed inhibition experiments by specifically blocking the 'a' and/or 'b' holes with peptides to determine whether 'B-b' interactions occur simultaneously to 'A-a' interactions within the same pair of interacting molecules.

Materials and methods

Materials

All reagents were of analytical grade and purchased from Sigma (St Louis, MO, USA) unless noted otherwise. Human plasma fibrinogen (FIB 1) and α-thrombin (HT 2970PA) were purchased from Enzyme Research Laboratories (Southbend, IN, USA). Batroxobin (*Batroxobin moojeni*) was obtained from CenterChem (Stamford, CT, USA). Peptides GPRP amide and GHRP amide were purchased from Bachem USA (Torrance, CA, USA) and Biopeptide Co. (San Diego, CA, USA). Peptide AHRPY amide [29] was synthesized by the Protein Chemistry Core Facility at the University of North Carolina at Chapel Hill.

Fibrinogen preparation

Fibrinogen was dialyzed against 20 mM HEPES, pH 7.4, 150 mM NaCl, 1 mM $CaCl_2$ buffer (HBSC), stored at −80 °C, thawed at 37 °C for 10 min and maintained at ambient temperature. Fibrinogen concentration was determined using an extinction coefficient of 1.51 at 280 nm for a 1 mg mL^{-1} solution [30].

NDSK fragment preparation

We prepared three different forms of NDSK fragments (Fig. 1B) based on described procedures [31,32]. Fibrin clots were formed by adding thrombin (1 U mL^{-1}) or batroxobin (1 BU mL^{-1}) to fibrinogen (10 mg mL^{-1}) and incubating for 24 h. The fibrin clot or fibrinogen (10 mg mL^{-1}) was dissolved in 70% formic acid and reacted with CNBr (1/1.5, w/w, protein/CNBr ratio). The reaction continued for 24 h at ambient temperature under nitrogen. Following dialysis against 5% acetic acid and 100 mM NaCl, NDSK was purified from fibrinogen, desA-NDSK from batroxobin-generated fibrin, and desAB-NDSK from thrombin-generated fibrin. Each fragment was purified by size-exclusion chromatography using two sequentially connected Superdex 200 prep grade HR16/50 columns (Pharmacia, Uppsala, Sweden), equilibrated with 5% acetic acid and 100 mM NaCl. Fragment fractions were pooled, concentrated using a 30 kDa molecular mass cut-off centrifugal filter device (Millipore, Bedford, MA, USA), dialyzed against 20 mM HEPES, pH 7.4, 150 mM NaCl buffer (HBS), and stored at −80 °C. The fragment concentrations were determined from the absorbance at 280 nm using the theoretical extinction coefficients for 1 mg mL^{-1} solutions, 0.74 for NDSK (Mr = 59 kDa), 0.78 for desA-NDSK (Mr = 56 kDa), and 0.82 for desAB-NDSK (Mr = 53 kDa).

Polyacrylamide gel electrophoresis (PAGE)

We performed native and SDS electrophoresis with an automated PHAST system (Pharmacia, Uppsala, Sweden), using the same 8–25% gradient polyacrylamide gels. Native gels were run using 0.25 M Tris, 0.88 M L-alanine pH 8.8 buffer for 280 Vh. SDS gels were run using 0.20 M Tricine, 0.20 M Tris, pH 8.1, 0.55% SDS buffer system for 76 Vh. Protein bands were visualized with Coomassie R250.

Analytical ultracentrifugation

Sedimentation equilibrium experiments were performed using a Beckman Optima XL-I analytical ultracentrifuge with a Ti50 8-hole rotor and six-sectored centerpieces. Samples of NDSK, desA-NDSK and desAB-NDSK (three different

concentrations of each fragment at 0.25, 0.50 and 0.75 ABS_{280}) were spun at 8064 ***g*** or at 13 628 ***g*** for 18 h at 25 °C. Absorbance scans at 280 nm were recorded every 2 h. Equilibrium was assumed when the difference between two consecutive absorbance profiles became zero. The meniscus-depletion method was employed to determine the absorbance offsets after over-speeding the samples at 50 400 ***g*** for 6 h. Equilibrium absorbance profiles were analyzed using Beckman XL-A/XL-I Analysis Software Version 4.0 and fit using both a single-species and a monomer-dimer model based on the Lamm equation [33]. Experiments with NDSK and desA-NDSK were performed twice, and the equilibrium constants averaged; with desAB-NDSK the experiment was performed once.

Surface plasmon resonance (SPR)

We prepared SPR sensorchips in house for use with a Biacore X (Biacore, Inc., Uppsala, Sweden) instrument using glass cover slips (Electron Microscopy Sciences, Washington, PA, USA) modified with hydrophobic self-assembled monolayers (SAMs), as described [34]. The HBSC flow rate was a constant 10 μL min^{-1} and a continuous flow of 25 °C buffer was maintained through the instrument at all times. After reaching a stable baseline (drift < 1 response U min^{-1}), 1 mg mL^{-1} fibrinogen in HBSC was flowed over the sensorchip surface for 600 s, the chip rinsed with HBSC for 300 s and then washed three times using the manufacturer's 'wash' command over an additional 300 s. The NDSK, desA-NDSK or desAB-NDSK samples were injected over the thoroughly rinsed adsorbed fibrinogen and the association/dissociation profiles were monitored for 600 s. Notably, we used 1 mg mL^{-1} fibrinogen to generate a closely-spaced monolayer of protein, minimizing conformational changes observed with monolayers formed from dilute solutions [35,36]. We measured the desA- and desAB-NDSK binding 600 s after completion of the fragment injection to avoid the complications associated with measuring and subtracting bulk refractive index shifts. Thus, steady-state measurements rather than kinetic analyses were used to determine equilibrium binding constants.

To obtain binding curves, fibrinogen deposition and fragment binding were repeated for a range of concentrations of desA-NDSK or desAB-NDSK fragments using a new sensorchip for each experiment. Profiles were normalized with respect to the amount of fibrinogen deposited during each binding experiment, correcting the SPR signal for the molecular mass difference of the fragments compared with fibrinogen. Experiments were designed to be independent of the concentration of fibrinogen molecules capable of binding fragments, which we assumed to be reproducible from sensorchip to sensorchip. The reproducibility of our data supported this assumption. The resulting normalized signal was expressed in units of binding ratios, representing an average number of fragment molecules bound per fibrinogen molecule. For desAB-NDSK, the normalized binding response was plotted against fragment concentration to generate a binding curve. For desA-NDSK, which exists in a monomer-dimer equilibrium in solution, we calculated the ratio of monomers to dimers at each desA-NDSK concentration using the centrifugation data and adjusted the total SPR signal for the binding of dimers to the adsorbed fibrinogen. The mass contribution of the second molecule in the dimer, which we assumed does not directly interact with adsorbed fibrinogen and therefore does not contribute to the affinity of desA-NDSK for fibrinogen, was subtracted from the total fragment binding. The resulting signal was the mass response of the monomers and one molecule of the dimer pair that was interacting directly with adsorbed fibrinogen. The final corrected signal from desA-NDSK molecules directly interacting with fibrinogen was plotted against fragment concentration to generate a binding curve. We performed peptide competition experiments in triplicate using GPRP, GHRP and AHRPY by incubating 25 μM desA-NDSK or desAB-NDSK with 4 mM of one or two peptides prior to injection over adsorbed fibrinogen.

Results

Purification of NDSK, desA-NDSK and desAB-NDSK fragments

The NDSK fragment of fibrinogen is composed of two copies each of Aα1-51, Bβ1-118, and γ1-78, all joined by 11 disulfide bonds. NDSK, containing intact FpA and FpB and thus no exposed polymerization knobs, was purified from a CNBr digest of fibrinogen. The fragments desA-NDSK, containing polymerization knobs 'A', and desAB-NDSK, containing polymerization knobs 'A' and 'B', were purified from the CNBr digest of desA- and desAB-fibrin, respectively. The ligand fragments, depicted in Fig. 1B, were generated and purified as described in the methods. A representative chromatogram of NDSK fragment purification is shown in Fig. 2. The reaction conditions generated two products, which appeared as a closely spaced doublet in sodium dodecyl-sulfate–polyacrylamide gel electrophoresis (SDS–PAGE) (for NDSK, the two top-most bands in Fig. 2 insert, indicated by the arrow in CNBr digest lane). Increasing the digest time (up to 48 h) or concentration of CNBr (up to 1/5, w/w, protein/CNBr ratio) did not change the appearance or yield of the NDSK species. Notably, doublets were present in the CNBr digests of fibrinogen, desA- and desAB-fibrin clots. We resolved the two products (Fig. 2 insert, NDSK lane) using size exclusion chromatography and, for all experiments, we used the form with the lower apparent molecular mass. These fragments ran as single bands in the presence of SDS with an apparent molecular mass of *c.* 67 kDa (Fig. 2, insert and Fig. 3B).

Characterization of NDSK fragments

The NDSK fragments were analyzed by both native and denatured polyacrylamide gel electrophoresis (PAGE). While both NDSK and desAB-NDSK appeared as single bands on the native gel, the desA-NDSK fragment appeared as two

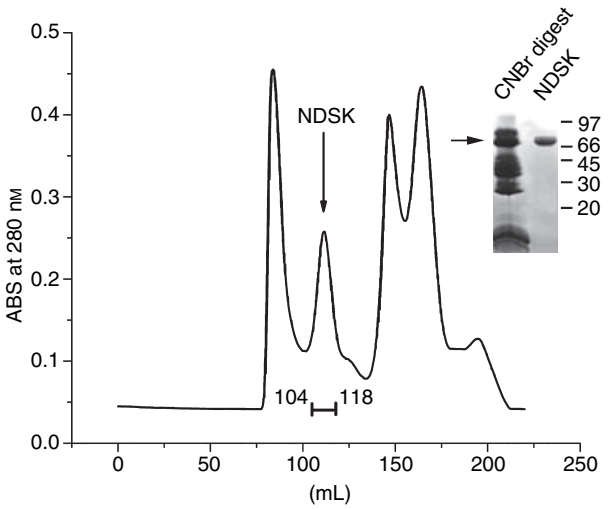

Fig. 2. Representative chromatogram of NDSK fragment purification using two sequentially connected Superdex 200 prep grade HR16/50columns. The position of the NDSK peak and the volume (mL) over which fragments were collected are identified by the horizontal bracket underneath the peak. The insert shows an 8–25% gradient sodium dodecylsulfate–polyacrylamide gel of the CNBr digest of fibrinogen with the NDSK bands denoted by an arrow and final purified NDSK fragment from the CNBr digest. The position of molecular mass markers (in kDa) is indicated on the right.

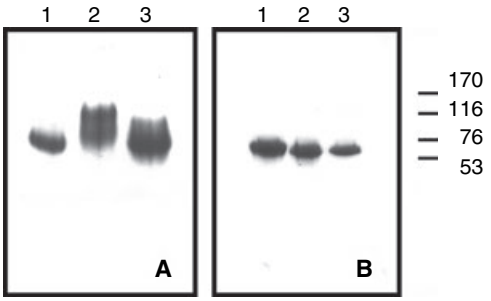

Fig. 3. Polyacrylamide gel electrophoresis analysis of NDSK (1), desA-NDSK (2) and desAB-NDSK (3) in a native 8–25% gradient polyacrylamide gel (A) and in a denatured [sodium dodecylsulfate (SDS)] 8–25% gradient polyacrylamide gel (B). The position of the molecular mass markers (in kDa) for the denatured SDS gel is indicated at the side of panel B.

bands, suggesting the presence of a higher molecular mass species (Fig. 3). In contrast, all three fragments ran as single bands during SDS–PAGE, (Fig. 3B). To characterize the fragments in solution, we performed analytical ultracentrifugation experiments of NDSK, desA-NDSK and desAB-NDSK in HBSC (see Fig. S1 in Supplementary material), as described in the methods. The equilibrium absorbance profiles were analyzed using both a single-species and a monomer-dimer model based on the Lamm equation [33]. The best fit was obtained with a monomer-dimer model using the calculated molecular weights of 59 kDa for NDSK, 56 kDa for desA-NDSK, and 53 kDa for desAB-NDSK monomers. From this fit, the equilibrium dissociation constants of complex formation were determined to be 25 μM for NDSK, 12 μM for desA-NDSK, and 46 μM for desAB-NDSK. Thus, under the conditions of our SPR experiments up to 60% of the desA-NDSK molecules were dimers, while essentially all NDSK and desAB-NDSK molecules were monomers.

NDSK binding experiments

Fragment binding to adsorbed fibrinogen was measured by SPR; a representative sensorgram is shown in Fig. 4. Fibrinogen was adsorbed at the hydrophobic surface of the methyl-terminated SAM upon flowing 1 mg mL^{-1} fibrinogen over the SPR sensor chip surface (Fig. 4A). The adsorption of fibrinogen resulted in monolayer coverage of the surface with a protein density of $6.0 \pm 0.9 \times 10^{-9}$ μg μm^{-2} calculated assuming 1 SPR response unit is equivalent to 1 pg mm^{-2} of protein surface coverage as described by Biacore. Because exposure of the adsorbed fibrinogen to an additional injection of 1 mg mL^{-1} fibrinogen did not result in additional adsorption (data not shown), we concluded the chip surface was completely covered. Because fibrinogen desorption from the surface during subsequent buffer flow was minimal (Fig. 4B), we concluded that fibrinogen molecules adhered to the SAM rather than to one another. The observed 6000 SPR response unit change correlated well with previous reports using similar conditions and instrumentation [34].

To determine the affinity constants for knob-hole interactions, two different knob-containing fragments were employed. The desA-NDSK fragment contained only the 'A' knob, while the desAB-NDSK fragment contained both the 'A' and 'B' knobs. We studied the binding of both knob-containing fragments in solution to holes in immobilized fibrinogen. Upon introduction of desAB-NDSK into the SPR flow cell, the fragment associated with the adsorbed fibrinogen as indicated by the increase in SPR response (Fig. 4C). After restoration of buffer flow (Fig. 4D) there was a continual, very small change in SPR response consistent with the slow dissociation of

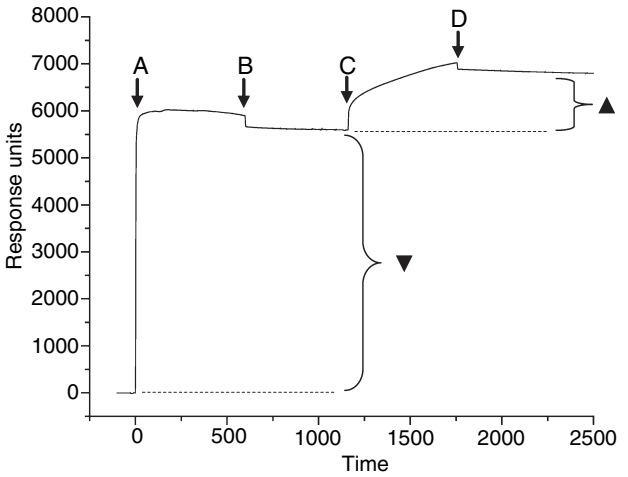

Fig. 4. Representative SPR sensorgram of response unit changes observed during (A) injection of 1 mg mL^{-1} fibrinogen, (B) restoration of buffer flow, (C) injection of 25 μM desAB-NDSK and (D) restoration of buffer flow. The maximum surface plasmon resonance response change for fibrinogen is identified by (▼) and for desAB-NDSK fragment by (▲).

desAB-NDSK. We observed a similar profile for desA-NDSK binding to fibrinogen. We obtained fragment-binding profiles over a concentration range of 0.1 to 22 μM for desAB-NDSK and 0.1 to 43 μM for desA-NDSK. The SPR responses were converted to binding ratios (BR), the average number of fragment molecules bound per fibrinogen molecule on the surface, using Eqn 1.

$$\text{Binding ratio} = \frac{\text{Fragment SPR response}}{\text{Fibrinogen SPR response}} \times \frac{\text{Mr (fibrinogen)}}{\text{Mr (fragment)}} \quad [1]$$

where fragment RU is the SPR response generated by the fragment bound to fibrinogen (▲ in Fig. 4), fibrinogen RU is the SPR response generated by the adsorption of fibrinogen (▼ in Fig. 4), Mr (fibrinogen) is the mass of fibrinogen (340 kDa), and Mr (fragment) is the mass of each corresponding fragment (desA-NDSK = 56 kDa and desAB-NDSK = 53 kDa). Because our ultracentrifugation and native PAGE data showed the desA-NDSK fragment self-associates, a correction was applied to account for the mass contribution of desA-NDSK dimers. The binding ratios obtained from Eqn 1 were adjusted using Eqn 2.

$$\text{Adjusted desA-NDSK BR} = \text{desA-NDSK BR} - \frac{\text{desA-NDSK BR} \times \%\ \text{desA-NDSK dimer}}{2} \quad [2]$$

The % desA-NDSK dimer was calculated for each desA-NDSK concentration using a dimer equilibrium dissociation constant of 12 μM. Finally, the desAB-NDSK binding ratios and desA-NDSK adjusted binding ratios were plotted as a function of desA- or desAB-NDSK concentration and the resulting binding curve for each NDSK fragment is shown in Fig. 5. The plotted data were fit using a single-site interaction binding model, as shown in Eqn 3.

$$\text{BR} = \frac{B_{\max}[\text{NDSK fragment}]}{K_d + [\text{NDSK fragment}]} \quad [3]$$

where $B_{\max}$ is the maximum binding signal, K_d is the equilibrium dissociation constant, and [NDSK fragment] is the concentration of the injected fragment in micromolar. We determined K_d values of 3.7 ± 0.7 μM for desAB-NDSK and 5.8 ± 1.1 μM for desA-NDSK binding to fibrinogen, which were not statistically different at the 95% confidence level according to a two-sided unpaired *t*-test ($P = 0.14$). The maximum binding was 2.3 ± 0.1 for desA-NDSK and 1.6 ± 0.1 for desAB-NDSK (Fig. 5).

Additional SPR experiments were conducted to verify the specificity and evaluate the individual contributions of 'A-a' and 'B-b' interactions. Firstly, we examined binding of the NDSK fragment with no active knobs. At 50 μM the binding of NDSK was < 15% of the desA-NDSK binding at 43 μM (see Fig. S2 in Supplementary material), demonstrating no significant binding in the absence of knobs. Secondly, peptide inhibitors of polymerization were employed to selectively inhibit either 'A-a' (GPRP) or 'B-b' (GHRP and AHRPY) interactions. DesA- or desAB-NDSK (25 μM) was incubated with the peptides, the mixture exposed to adsorbed fibrinogen, and the SPR signal assessed 1200 s after injection. When desAB-NDSK was incubated with GHRP and GPRP individually, the binding was decreased by 48% and 89%, respectively, compared with desAB-NDSK alone (Fig. 6A). Because crystallography studies showed GHRP can bind in both the 'a' and 'b' holes [37], we also examined inhibition with AHRPY, which binds exclusively in the 'b' hole [29]. The results with AHRPY were the same as with GHRP, desAB-NDSK binding decreased 52% compared with desAB-NDSK alone (see Fig. S3 in Supplementary material). When the equimolar mixture of GHRP and GPRP was incubated with desAB-NDSK the binding ratio fell below zero, likely due to both the loss of desAB-NDSK binding and a slight desorption of fibrinogen. The small decrease in SPR signal resulting from fibrinogen desorption was determined to be < 2% over the course of each experiment and was not detectable for any of the other fragment/peptide mixtures because the increase in signal due to fragment binding obscured the decrease in signal due to fibrinogen desorption. Similar to desAB-NDSK with GPRP, we observed an 84% decrease in binding when desA-NDSK was incubated with GPRP (Fig. 6B). Incubation of desA-NDSK with GHRP or AHRPY did not result in inhibition, but rather a slight increase in binding compared with desA-NDSK alone. Finally, the addition of an equimolar mixture of GHRP and GPRP to desA-NDSK resulted in an 89% decrease in desA-NDSK binding. Collectively, these results demonstrate that the binding of desA- and desAB-NDSK to fibrinogen was promoted by specific knob-hole interactions and that 'B-b' knob-hole interactions contribute to the binding of desAB-NDSK to surface-bound fibrinogen.

Discussion

The design of our experiments allowed measurement of the affinities for knob-hole interactions between two molecules, either 'A-a' alone or 'A-a' and 'B-b' together, in the absence of the other interactions that occur during polymerization. Although the affinities we determined, 5.8 ± 1.1 μM and 3.7 ± 0.7 μM, were not significantly different from one another, the higher affinity for the desAB-NDSK suggests both 'A-a' and 'B-b' interactions contribute to the binding. This suggestion was confirmed by the peptide inhibition studies, which showed that both knob-hole pairs participate in desAB-NDSK binding to immobilized fibrinogen. We observed at least an 84% decrease in both desA- and desAB-NDSK binding to fibrinogen in the presence of GPRP, demonstrating that 'A-a' interactions are important to the binding of both fragments. Moreover, GHRP and

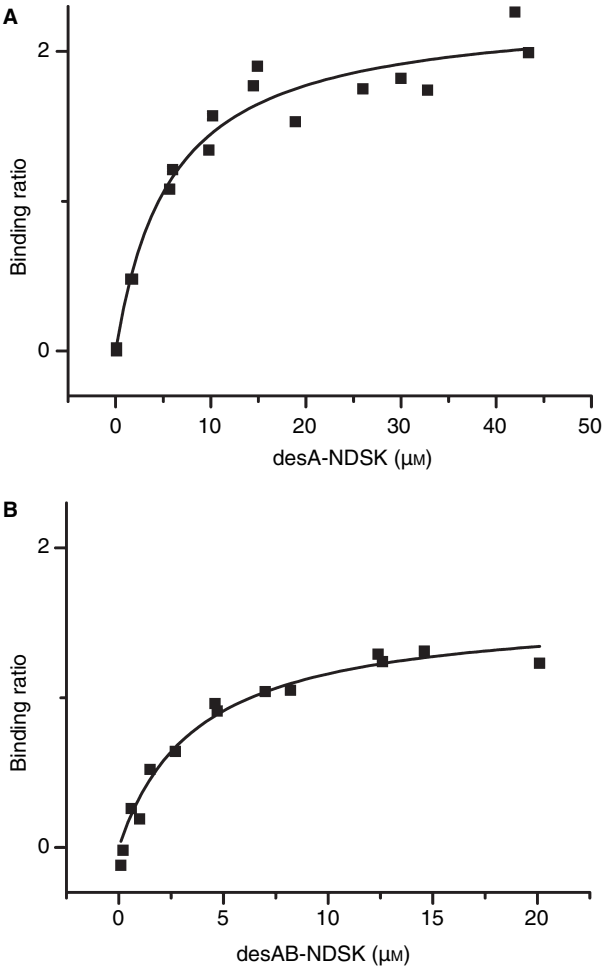

Fig. 5. Binding curves for (A) desA-NDSK and (B) desAB-NDSK binding to 1 mg mL^{-1} fibrinogen adsorbed to a hydrophobic-terminated self-assembled monolayer as determined by surface plasmon resonance. The solid curves are the best fits obtained using Eqn 3.

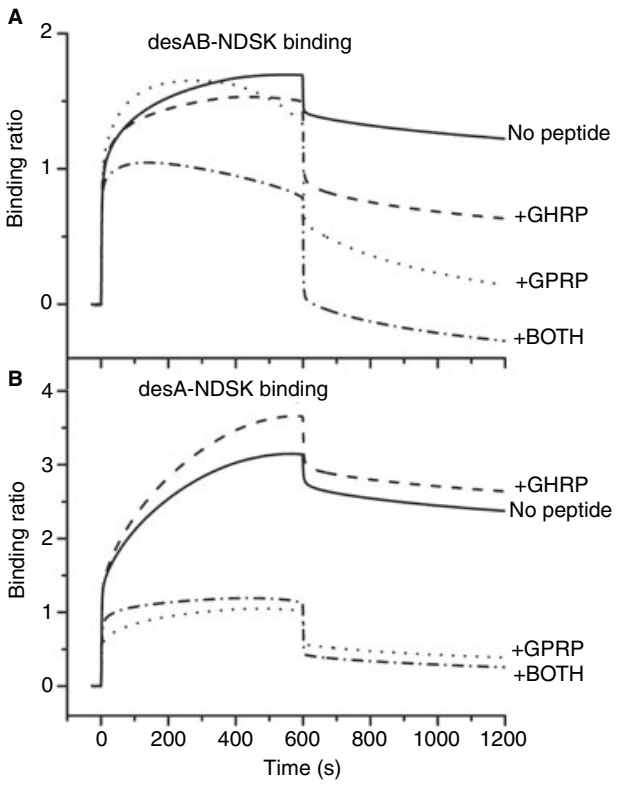

Fig. 6. Surface plasmon resonance sensorgrams showing the average binding of (A) 25 μM desAB-NDSK (solid line) and (B) 25 μM desA-NDSK (solid line), in the presence of 4 mM GHRP (dashed line), 4 mM GPRP (dotted line), and equimolar mixture (BOTH) of GHRP and GPRP (dashed and dotted line) to adsorbed fibrinogen.

AHRPY competed solely with desAB-NDSK, indicating that 'B-b' interactions participate in desAB-NDSK but not desA-NDSK binding to immobilized fibrinogen. Finally, the GHRP/GPRP mixture decreased desAB-NDSK binding more than GPRP alone, as expected if 'B-b' interactions contributed to this interaction. Taken together these data strongly support the conclusion that 'B-b' interactions participate in the binding of desAB-NDSK to immobilized fibrinogen. This finding differs from that obtained in recent laser tweezers studies where GPRP, but not GHRP, inhibited interactions between desAB-NDSK and fibrinogen [22]. 'B-b' interactions were detected in laser tweezers experiments only under conditions where 'A-a' interactions were impaired or excluded [23]. The difference between our SPR results and the laser tweezers data likely reflects the inherent differences between the methods. For example, 'B-b' interactions may occur subsequent to 'A-a' interactions and thus are not detected in the forced dissociations of the laser tweezers binding studies. Alternatively, the nature of the immobilized species, directly adsorbed fibrinogen in the SPR experiments or covalently immobilized fibrinogen in the laser tweezers experiments, may alter availability of the 'b' hole.

The affinities we determined, 5.8 ± 1.1 μM and 3.7 ± 0.7 μM, are remarkably similar to those determined for fragment D binding to suspended desAB-fibrin fragments that were produced by sonication, 2.4 μM [38]. This similarity suggests that the affinities determined by SPR are analogous to those found in solution. Interactions between fibrinogen and suspended desAB-fibrin fragments were even stronger, 56 nM, as anticipated if one fibrinogen molecule binds to fibrin through multiple sites (i.e. the two D domains) [38]. Recently, Ugarova and colleagues determined a similar affinity, 1.47 ± 0.26 μM, using SPR to measure soluble fibrinogen binding to covalently immobilized fibrin molecules [39]. The similarity of these measurements suggests that our studies measure the interactions that mediate fibrin monomer binding to a single D domain of intact fibrinogen. Other investigations have examined the individual 'A-a' and 'B-b' interactions using peptides that mimic the 'A' and 'B' knobs, GPRP and GHRP. In the presence of 2 mM calcium they found K_d's of 20 μM for GPRP and 16 μM for GHRP [40]. These affinities are somewhat weaker than the affinities we determined for the larger desA- and desAB-NDSK fragments, which likely reflects the entropy costs associated with

restraining the conformations of the smaller molecules. Considered with the published data [19,38,40,41], the values we determined by SPR are rational, indicating that our data reflect the affinities of the 'A-a' and 'B-b' interactions as they occur in fibrin polymers.

The observation that desAB-NDSK binds fibrinogen through both 'A-a' and 'B-b' interactions infers that both sets of interactions can occur between the same two fibrin molecules in a polymer. That is, 'A-a' and 'B-b' interactions may both support protofibril formation. A model where 'B-b' interactions occur within protofibrils was also inferred from previous studies using recombinant fibrinogens with substitutions in the high-affinity calcium binding site in γC [21,42]. Thrombin-catalyzed polymerization of these fibrinogens was severely impaired; this polymerization was abolished by GHRP; and batroxobin-catalyzed polymerization was undetectable. Similarly, Okumura and his colleagues have recently found: that substitutions in the 'a' hole markedly impair thrombin-catalyzed polymerization; that this polymerization is abolished by GHRP; and that anchrod-catalyzed polymerization of these variants was undetectable [43]. Consideration of our SPR binding studies together with the polymerization of these variant fibrinogens indicates that (i) both 'A-a' and 'B-b' interactions can support protofibril formation, (ii) 'A-a' interactions are higher affinity than 'B-b' and on their own can support nearly normal polymerization, and (iii) 'B-b' interactions are lower affinity than 'A-a' but are sufficient to support delayed polymerization.

We also discovered that desA-NDSK, and to a much lower degree NDSK and desAB-NDSK, form dimers in solution. Importantly, the dimerization of fragments does not preclude their binding to fibrinogen. Our observation suggests that the desA-NDSK monomers comprising the dimer are connected via regions of the molecule that do not interfere with the 'A' knob and subsequent 'A-a' interactions. A recent laser tweezers study, which examined interactions between pairs of NDSK fragments, indicates that FpB mediates desA-NDSK dimerization. These studies showed interactions between two desA-NDSK molecules. These interactions were lost when FpB was removed from one of the molecules, indicating they are dependent on the presence of fibrinopeptide B [32]. The biological significance of desA-NDSK dimerization is currently unknown.

In conclusion, we found in SPR binding studies that both 'A-a' and 'B-b' interactions participate in the binding of desAB-NDSK to fibrinogen, and that the affinity of desA-NDSK binding was not markedly different from desAB-NDSK binding, indicating that 'A-a' interactions are strong. These findings suggest that 'B-b' interactions can occur alongside 'A-a' interactions when both the 'B' knob and 'b' hole are available.

Acknowledgements

We thank N. Okumura for helpful discussions and A. Wolberg for assistance with statistical analyses. This work was supported by National Institutes of Health grant HL-31048 (STL) and National Science Foundation grant CHE-0349091 (MHS) and the University of North Carolina Molecular and Cellular Biophysics training program supported by NIGMS training grant 5-T32-GM08570UNC.

Disclosure of Conflict of Interests

The authors state that they have no conflict of interest.

Supplementary Material

The following supplementary material is available for this article:

Fig. S1. Analytical ultracentrifugation sedimentation data for NDSK, desA- and desAB-NDSK. (A) Curve-fitting residuals and (B) equilibrium absorbance profiles.
Fig. S2. SPR sensorgrams showing the binding of 43 μM desA-NDSK (dashed line) and 50 μM NDSK (solid line) to adsorbed fibrinogen.
Fig. S3. SPR sensorgrams showing the average binding of 25 μM desA-NDSK and 4 mM AHRPY (dashed line) and des-AB-NDSK and 4 mM AHRPY (solid line) to adsorbed fibrinogen.

This material is available as part of the online article from: http://www.blackwell-synergy.com/doi/abs/10.1111/j.1538-7836.2007.02774.x (This link will take you to the article abstract).

Please note: Blackwell Publishing are not responsible for the content or functionality of any supplementary materials supplied by the authors. Any queries (other than missing material) should be directed to the corresponding author for the article.

References

1 Laurens N, Koolwijk P, De Maat MPM. Fibrin structure and wound healing. *J Thromb Haemost* 2006; **4**: 932–9.
2 Weisel JW. Fibrinogen and fibrin. *Adv Protein Chem* 2005; **70**: 247–99.
3 Henschen A, Lottspeich F, Kehl M, Southan C. Covalent structure of fibrinogen. *Ann N Y Acad Sci* 1983; **408**: 28–43.
4 Spraggon G, Everse SJ, Doolittle RF. Crystal structures of fragment D from human fibrinogen and its crosslinked counterpart from fibrin. *Nature* 1997; **389**: 455–62.
5 Pratt KP, Cote HCF, Chung DW, Stenkamp RE, Davies EW. The primary fibrin polymerization pocket – three-dimensional structure of a 30-kDa C-terminal gamma chain fragment complexed with the peptide Gly-Pro-Arg-Pro. *Proc Natl Acad Sci USA* 1997; **94**: 7176–81.
6 Everse SJ, Spraggon G, Veerapandian L, Riley M, Doolittle RF. Crystal structure of fragment double-D from human fibrin with two different bound ligands. *Biochemistry* 1998; **37**: 8637–42.
7 Laurent TC, Blomback B. On the significance of the release of two different peptides from fibrinogen during clotting. *Acta Chem Scand* 1958; **72**: 1875–7.
8 Blomback B, Blomback M, Edman P, Hessel B. Human fibrinopeptides. Isolation, characterization and structure.. *Biochim Biophys Acta* 1966; **115**: 371–96.

9 Laudano AP, Doolittle RF. Synthetic peptide derivatives that bind to fibrinogen and prevent the polymerization of fibrin monomers. *Proc Natl Acad Sci USA* 1978; **75**: 3085–9.

10 Hantgan RR, Hermans J. Assembly of fibrin. A light scattering study. *J Biol Chem* 1979; **254**: 11272–81.

11 Olexa SA, Budzynski AZ. Localization of a fibrin polymerization site. *J Biol Chem* 1981; **256**: 3544–9.

12 Yang Z, Mochalkin I, Doolittle RF. A model of fibrin formation based on crystal structures of fibrinogen and fibrin fragments complexed with synthetic peptides. *Proc Natl Acad Sci USA* 2000; **97**: 14156–61.

13 Hurlet-Jensen A, Cummins HZ, Nossel HL, Liu CY. Fibrin polymerization and release of fibrinopeptide B by thrombin. *Thromb Res* 1982; **27**: 419–27.

14 Higgins DL, Lewis SD, Shafer JA. Steady state kinetic parameters for the thrombin-catalyzed conversion of human fibrinogen to fibrin. *J Biol Chem* 1983; **258**: 9276–82.

15 Ruf W, Bender A, Lane DA, Preissner KT, Selmayr E, Muller-Berghaus G. Thrombin-induced fibrinopeptide B release from normal and variant fibrinogens: influence of inhibitors of fibrin polymerization. *Biochim Biophys Acta* 1988; **965**: 169–75.

16 Weisel JW, Veklich Y, Gorkun O. The sequence of cleavage of fibrinopeptides from fibrinogen is important for protofibril formation and enhancement of lateral aggregation in fibrin clots. *J Mol Biol* 1993; **232**: 285–97.

17 Shimizu A, Ferry JD. Clots of beta-fibrin. Viscoelastic properties, temperature dependence of elasticity, and interaction with fibrinogen-binding tetrapeptides. *Biophysical J* 1988; **53**: 311–8.

18 Shen LL, Hermans J, McDonagh J, McDonagh RP. Role of fibrinopeptide B release: comparison of fibrins produced by thrombin and Ancrod. *Amer J Pathol* 1977; **232**: H629–33.

19 Shainoff JR, Dardik BN. Fibrinopeptide B in fibrin assembly and metabolism: physiologic significance in delayed release of the peptide. *Ann N Y Acad Sci* 1983; **408**: 254–68.

20 Mosesson MW, DiOrio JP, Muller MF, Shainoff JR, Siebenlist KR, Amrani DL, Homandberg GA, Soria J, Soria C, Samama M. Studies on the ultrastructure of fibrin lacking fibrinopeptide B (beta-fibrin). *Blood* 1987; **69**: 1073–81.

21 Lounes KC, Ping L, Gorkun OV, Lord ST. Analysis of engineered fibrinogen variants suggests that an additional site mediates platelet aggregation and that "B-b" interactions have a role in protofibril formation. *Biochemistry* 2002; **41**: 5291–9.

22 Litvinov RI, Gorkun OV, Owen SF, Shuman H, Weisel JW. Polymerization of fibrin: specificity, strength, and stability of knob-hole interactions studied at the single-molecule level. *Blood* 2005; **106**: 2944–51.

23 Litvinov RI, Gorkun OV, Galanakis DK, Yakovlev S, Medved L, Shuman H, Weisel JW. Polymerization of fibrin: direct observation and quantification of individual B:b knob-hole interactions. *Blood* 2007; **109**: 130–8.

24 Bale MD, Muller MF, Ferry JD. Effects of fibrinogen-binding tetrapeptides on mechanical properties of fine fibrin clots. *Proc Natl Acad Sci USA* 1985; **82**: 1410–3.

25 Shimizu A, Schindlauer G, Ferry JD. Interaction of the fibrinogen-binding tetrapeptide Gly-Pro-Arg-Pro with fine clots and oligomers of alpha-fibrin; comparisons with alpha beta-fibrin. *Biopolymers* 1988; **27**: 775–88.

26 Okumura N, Gorkun OV, Terasawa F, Lord ST. Substitution of the gamma-chain Asn308 disturbs the D:D interface affecting fibrin polymerization, fibrinopeptide B release, and FXIIIa-catalyzed cross-linking. *Blood* 2004; **103**: 4157–63.

27 Matsuda M, Baba M, Morimoto K, Nakamikawa C. "Fibrinogen Tokyo II". An abnormal fibrinogen with an impaired polymerization site on the aligned DD domain of fibrin molecules. *J Clin Invest* 1983; **72**: 1034–41.

28 Gorkun OV, Veklich YI, Medved LV, Henschen AH, Weisel JW. Role of the alpha C domains of fibrin in clot formation. *Biochemistry* 1994; **33**: 6986–97.

29 Doolittle RF, Chen A, Pandi L. Differences in binding specificity for the homologous gamma- and beta-chain "holes" on fibrinogen: exclusive binding of Ala-His-Arg-Pro-amide by the beta-chain hole. *Biochemistry* 2006; **45**: 13962–9.

30 Mihalyi E. Physicochemical studies of bovine fibrinogen. IV. Ultraviolet absorption and its relation to the structure of the molecule. *Biochemistry* 1968; **7**: 208–23.

31 Blomback B, Hessel B, Iwanaga S, Reuterby J, Blomback M. Primary structure of human fibrinogen and fibrin. I. Clevage of fibrinogen with cyanogen bromide. Isolation and characterization of NH 2 -terminal fragments of the ("A") chain. *J Biol Chem* 1972; **247**: 1496–512.

32 Gorkun OV, Litvinov RI, Veklich YI, Weisel JW. Interactions mediated by the N-terminus of fibrinogen's Bβ chain. *Biochemistry* 2006; **45**: 14843–52.

33 McRorie DK, Voelker PJ. *Self-Associating Systems in the Analytical Centrifuge*. Palo Alto, California: Beckman Instruments, Inc., 1993.

34 Evans-Nguyen KM, Tolles LR, Gorkun OV, Lord ST, Schoenfisch MH. Interactions of thrombin with fibrinogen adsorbed on methyl-, hydroxyl-, amine-, and carboxyl-terminated self-assembled monolayers. *Biochemistry* 2005; **44**: 15561–8.

35 Sit PS, Marchant RE. Surface-dependent conformations of human fibrinogen observed by atomic force microscopy under aqueous conditions. *Thromb Haemost* 1999; **82**: 1053–60.

36 Agnihotri A, Siedlecki CA. Time-dependent conformational changes in fibrinogen measured by atomic force microscopy. *Langmuir* 2004; **20**: 8846–52.

37 Kostelansky MS, Bolliger-Stucki B, Betts L, Gorkun OV, Lord ST. Bβ Glu397 and Bβ Asp398 but not Bβ Asp432 are required for "B:b" interactions. *Biochemistry* 2004; **43**: 2465–74.

38 Husain SS, Weisel JW, Budzynski AZ. Interaction of fibrinogen and its derivatives with fibrin. *J Biol Chem* 1989; **264**: 11414–20.

39 Lishko VK, Burke T, Ugarova T. Antiadhesive effect of fibrinogen: a safeguard for thrombus stability. *Blood* 2007; **109**: 1541–9.

40 Laudano AP, Doolittle RF. Influence of calcium ion on the binding of fibrin amino terminal peptides to fibrinogen. *Science* 1981; **212**: 457–9.

41 Chtcheglova LA, Vogel M, Gruber HJ, Dietler G, Haeberli A. Kinetics of the interaction of desAABB-fibrin monomer with immobilized fibrinogen. *Biopolymers* 2006; **83**: 69–82.

42 Lord ST, Gorkun OV. Insight from studies with recombinant fibrinogens. *Ann N Y Acad Sci* 2001; **936**: 101–16.

43 Okumura N, Terasawa F, Haneishi A, Fujihara N, Hirota-Kawadobora M, Yamauchi K, Ota H, Lord ST. B:b interactions are essential for polymerization of variant fibrinogens with impaired holes 'a'. *J Thromb Haemost* 2007; **5**: 2352–9.